文章编号：1001-9014(2022)01-0311-06

DOI:10.11972/j.issn.1001-9014.2022.01.027

Design, fabrication and cold test of a high efficiency folded groove waveguide for w-band sheet beam TWT

TIAN Yan-Yan[1], WANG He-Xin[2], SHI Xian-Bao[3], LI Xin-Yi[4], GONG Yu-Bin[2], HE Wen-Long[1*]

(1. Free Electron Terahertz and Nanobeam Laboratory Shenzhen University, Shenzhen 518000, China;
2. School of Electronic Science and Engineering, University of Electronic Science and Technology of China, Chengdu 610054, China;
3. Ceyear Technologies Co., Ltd, Qingdao 266400, China;
4. Nanjing Sanle Electronic Group Co., Ltd; Nanjing 210008, China)

Abstract: In this paper, a design, fabrication and cold test of a high efficiency folded groove waveguide (FGW) for w-band (85~110GHz) sheet beam traveling wave tube (TWT) is proposed. One stage phase velocity taper (OSPVT) was used in the FGW to enhance the electronic efficiency of a millimeter-wave sheet beam TWT. The OSPVT was realized via a change of the period of the FGW. Three FGWs with and without OSPVT were fabricated and their measured s-parameters demonstrate good transmission characteristics and wide bandwidth. Moreover, wave dispersions and phase velocities of the unchanged and OSPVT FGWs were obtained from measured transmission phases. 3-D particle-in-cell simulations of beam-wave interaction predicted that the proposed TWT with an OSPVT of twenty half periods could output a saturated power of 240 W at 95 GHz, which is about 70 W higher than the case of without OSPVT. Meanwhile, the application of the OSPVT improves the electronic efficiency in the whole operating frequency range of 85~110 GHz, with a maximum efficiency enhancement of about 47% in the vicinity of 95 GHz.

Key words: folded groove waveguide, once stage phase velocity taper, millimeter-wave traveling wave tube, electronic efficiency enhancement, high-power source

高效率曲折槽波导毫米波行波管设计、制造和冷测

田艳艳[1], 王禾欣[2], 石先宝[3], 李新义[4], 宫玉彬[2], 何文龙[1*]

(1. 电子与信息工程学院,深圳大学,广东 深圳 518000;
2. 电子科学与工程学院,电子科技大学,四川 成都 610054;
3. 中国电科思仪科技股份有限公司,山东 青岛 266400;
4. 南京三乐电子信息产业集团有限公司,江苏 南京 210008)

摘要:本文提出一种适用于工作在毫米波段(85~110 GHz)的带状注高效率曲折槽波导毫米波行波管,并进行了参数优化设计、加工制造和冷测实验研究。曲折槽波导首次采用一次改变周期相速跳变技术提高带状注毫米波行波管电子互作用效率。文中加工制造了三种不同周期个数(包含相速跳变和均匀相速两种类型)的曲折槽波导,并进行了S参数测试,其结果表明应用一次相速跳变技术的曲折槽波导具有良好的传输特性和较宽的带宽。此外,通过测量三种不同周期个数曲折槽波导的相位传输得到了不同周期p_0和p_1的色散曲线,其结果证明通过仿真得到的色散曲线和测量得到的色散曲线相吻合。文中注波互作用三维粒子模拟结果表明:当曲折槽波导慢波结构末端20个半周期采用一次相速跳变技术时,在频点95 GHz处输出饱和功率达到240 W,比同等条件下的均匀相速曲折槽波导行波管在95 GHz处高70 W。同时,曲折槽波导行波管采用一次

Received date: 2021-07-09, **revised date**: 2021-08-04 **收稿日期**:2021-07-09,**修回日期**:2021-08-04

Foundation items: Supported by the National Natural Science Foundation of China (62001297, 61921002 and 61988102) and Shenzhen Science and technology (JCYJ 2020019105415835 and KQTD 20200820113046084)

Biography: TIAN Yanyan (1985-), female, associate professor. Current research interests include Microwave and Terahertz sensor. E-mail: tyy5586561@163.com

* **Corresponding author**: E-mail: wenlong.he@szu.edu.cn

相速跳变技术在频带85~110 GHz范围内电子效率明显得到提高,并且在95 GHz处最大电子效率提高了47%。

关 键 词:曲折槽波导;一次相速跳变;毫米波行波管;强电子效率;高功率源

中图分类号:TN124 **文献标识码**: A

Introduction

High power, wide bandwidth, high efficiency and high frequency electromagnetic radiation sources are in urgent demand, especially when the operating frequencies increase into the millimeter wave and terahertz ranges[1-3]. Higher power terahertz devices enable longer transmission distance and higher data-rate capability for wireless communications. For example, satellite communications are projected to use w-band (70~110 GHz)[4-5]. Vacuum electronic devices have high electronic efficiencies with a flexible manner without scattering phenomenon due to the vacuum environment, which are ideal for millimeter wave generations and amplifications. Therefore, vacuum electronic devices have strong advantages over solid state electronic devices, when the operating frequency is in the millimeter wave and higher terahertz band. Traveling wave tubes (TWT) are one of the most used vacuum electronic devices due to its capabilities of power and bandwidth.

However, high power amplifiers in sub-terahertz and terahertz frequency ranges are still lacking. A slow wave structure (SWS) is a core component of TWT devices and plays a crucial role in their performances, whilst also playing an important role in other large facilities such as linear synchrotron radiation light sources[6]. As the frequency increases, the commonly used SWSs, such as helix and coupled cavity, encounter the problems of power capacity, heat dissipation and micron-size manufacture. Folded waveguides have shown the characteristics of combined capabilities of high power and wide frequency bandwidth, as well as operability compared to traditional helix and coupled cavity structures. The first TWT based on a folded waveguide (FW) was studied by Waterman in 1979. Since then, a great deal of experimental and theoretical studies on FW-TWT have been published and several modified FWs were proposed for improving the performance of FW-TWTs[7-15]. However, FW will affect the electromagnetic field in the waveguide because the circular electron beam channel is made in the waveguide wall lending to increase reflection of FW and reduce its power capacity in the light of engineering.

In order to further improve TWT's performance in power, efficiency and bandwidth in the millimeter-wave and terahertz band, one stage phase velocity taper (OSPVT) was studied and applied to a Folded Groove Waveguide (FGW) TWT for the first time in this paper. The technique could be considered to be a simple version of Dynamic Velocity Technology (DVT) which has been used in the helix TWTs[16-17]. This idea could be applied to a variety of TWTs, such as those based on FWs or staggered double grating structures. FGW is suitable structure to operate in a sheet beam and the manufacture of the beam channel is unnecessary, which the electromagnetic field distribution affected in FGW is no longer existing. Therefore, FGW possesses higher power capability than FW, from the stand point of practical view. The FGW, as a kind of SWS, has been proposed for its low transmission loss because the ohmic loss on its wall is much lower than that of an FW[18]. Moreover, the loss coefficient of an FGW decreases with the increase in the frequency[19-20], which would be helpful for a terahertz TWT. Various FGWs with the cross-sections in the form of rectangular, V-, double ridge and ridge-loaded shapes have been studied[21-24].

The article is composed as follows. Section 1 contains the theoretical analysis of the phase velocity of the wave in FGWs and the principle of DVT. Section 2 presents the manufacture of the FGWs and their measured transmission and dispersion characteristics. The simulated performance of a high power millimeter-wave FGW-TWT exploiting OSPVT is presented in Section 3. Finally a brief summary is given in this paper.

1 Theory analysis

A schematic diagram of the FGW with sheet electron beam is shown in Fig. 1. The waveguide is formed between the two plates (1 and 2), both of which have a folded waveguide (3).

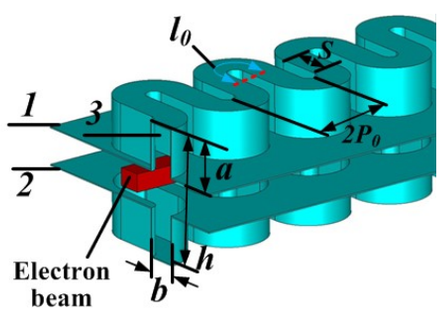

Fig. 1 The schematic diagram of the FGW with sheet electron beam present.

图1 带状电子束曲折槽波导示意图

Suppose the half-period of the FGW is P_0, which was designed to support a wave of an appropriate phase velocity V_{p0} to efficiently interact with an electron beam with velocity U_0. After electrons loosing enough energy their reduced velocity would be no longer in synchronism with the wave, and hence, wave growth would stop. However, at that moment if the phase velocity of the wave is adjusted to a degree so that it continues to match with the reduced electron velocity, then interaction could in principle continue to extract energy from the electrons and wave continue to grow, hence, improve the electron

efficiency of the TWT. In this paper the phase velocity of the electromagnetic wave is changed once by changing the half-period of the latter part of the FGW once, i. e. OSPVT, in the operating frequency. This extends the synchronous condition between the wave and the electron beam, transferring more energy from electrons to wave, hence improving the output power and electronic efficiency. When taking no account of the corner reflection and coupling between adjacent grooves, the analysis of the dispersion of the FGW is similar to that of an FW. The unchanged FGW has a curved groove length l_0 and a half period P_0. The OSPVT FGW has a curved groove length l_1 and a half period P_1. The length of the straight part is set to be s and defining the phase constant of the fundamental mode β_0 and its nth spatial harmonic β_{n0}, the phase velocity of the fundamental mode V_{p0} and its nth spatial harmonic V_{pn0}, then the following equations could be derived.

$$l_0 = \frac{\pi P_0}{2} + S \quad , \quad (1)$$

$$\beta_{n0} P_0 = \beta_0 l + (2n + 1)\pi \quad . \quad (2)$$

In formula (2), $\beta = \sqrt{k^2 - k_c^2}$, is the cutoff wave number and k is the wave number.

$$\frac{V_{pn0}}{c} = \left(l_0 \sqrt{1 - (\frac{k_c}{k})^2} + \frac{(2n + 1)\pi}{k} \right)^{-1} P_0 \quad , \quad (3)$$

here c is velocity of light, from Eq. (3) V_{Pn0} is a monotone function of half-period P_0. Hence, the phase velocity of the fundamental mode decreases as P_0 reduces. Only when the electron beam velocity U_0 is slightly faster than phase velocity of the wave V_{p0}, can the electron energy be transferred to waves. Supposing the electron beam velocity become U_1 when the beam-wave synchronization is about to lose, then electron energy transfer ratio is defined as $\eta = (U_0 - U_1)/U_0$. In order to maintain the synchronization condition, the electromagnetic wave phase speed V_{p0} needs to reduce as the electron velocity U_0 decreases to U_1. This decrease in speed of the electromagnetic wave phase speed V_{p0} is defined as Δ. Then we have:

$$\Delta = V_{p0} - V'_{p0} = \frac{\eta U_0}{1 + cB} \quad , \quad (4)$$

here $B = \frac{U_0 - V_{p0}}{CV_{p0}}$ is pierce velocity parameter[25].

Hence, by properly adjusting the phase velocity of the wave in the latter part of the FGW, the synchronous condition between the wave and electron velocity could maintain.

2 Experiments and discussions

As satellite communications plan to use w-band in the near future, a high power high efficiency folded groove waveguide millimeter-wave TWT based on OSPVT was designed (85~110 GHz). Fig. 2 (a) is a picture of the upper and lower half of the FGW machined by a high-speed CNC milling machine. The FGW with its input and output couplers was formed by assembling the two half with the help of eight screws and four location pins. The FGW with integrated input/output couplers includes two sections: a FGW section in the green box has unchanged half-period P_0 and an OSPVT section of 14 half-periods in the blue box with reduced period P_1. The dimensions of the structure are listed in Table 1.

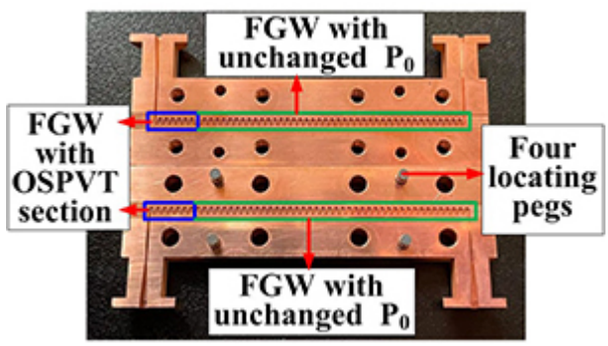

(a)

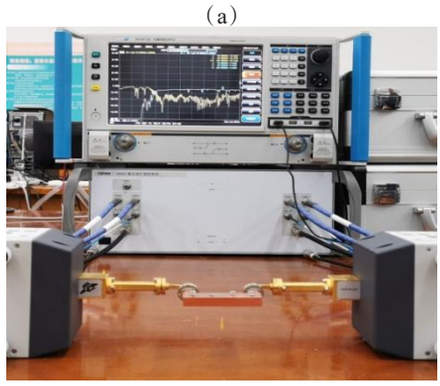

(b)

Fig. 2 (a) A photo showing the upper and lower half of the FGWs with in/out-puts, (b) setup for the cold test of the FGWs.
图2 (a) 带有输入输出结构的曲折槽波导上下部件照片, (b) 曲折槽波导冷测实验装置

Table 1 The parameter values of the FGWs
表1 曲折槽波导结构参数

Parameters	Description	Values(mm)
a	The depth of folded waveguide region	0. 82
b	The width of folded waveguide region	0. 35
s	The length of straight aveguide	0. 5
h	The height of FWG	1. 88
P_0	half-period FGW without OSPVT	0. 6
P_1	half-period FGW with OSPVT	0. 588

The setup for the cold test of the FGWs with and without OSPVT sections is shown in Fig. 2 (b). The S-parameters were measured by a vector network analyzer (Ceyear: AV3672E) with millimeter wave frequency extending module (Ceyar: 3640A). Simulated and measured s-parameters are displayed in Fig. 3. The simulated and measured reflection S_{11} were below -13 dB in the frequency range of 85 to 110 GHz. It can be seen from Fig. 3 that the measured curve of the reflection S_{11} is not perfectly consistent with the simulated one, this is be-

cause of the reflection of the windows in the input and output couplers. When an effective conductivity of 3.6*10^7 was used, the simulated transmission coefficient S_{21} agreed well with the measured one. Both the simulations and the measurements verified that the proposed FGW has good transmission characteristics and a wide bandwidth.

The electric field in the FGW is similar to that of TE_{11} mode in the circular waveguide. The measured wrapped phase of the operating mode in three FGWs is shown in Fig. 4. Fig. 4 shows the measured phase change of transmission (S_{21}) as a function of frequency for three structures: "structure a" has totally 98 half periods, 84 P_0 and 14 P_1; "structure b" 84 P_0, and "structure c" 58 P_0. All three structures have the same input and output couplers. Therefore, the phase change of the wave passing through the OSPVT section ($14*P_1$) could be obtained by taking the phase difference between case b and a. Similarly, the phase change of the wave of $26*P_0$ could be obtained by taking the difference between case c and b. The phase information was firstly unwrapped, then the differences between the unwrapped phases used to calculate the normalized phase velocity of the operating wave in FGWs with period P_0 and P_1 are shown in Fig. 5. It can be seen from Fig. 5 that the measured normalized phase velocities are in very good agreement with the simulated ones.

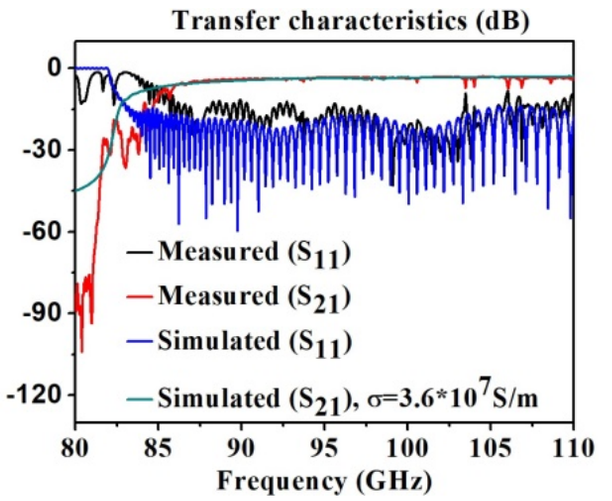

Fig. 3 The simulated and measured s-parameters of the FGW.
图3 仿真和测试曲折槽波导的S参数

3 Simulation of beam-wave interactions

In order to evaluate the performance of OSPVT, a high power high efficiency FGW millimeter-wave TWT based on OSPVT technology was designed, and it was

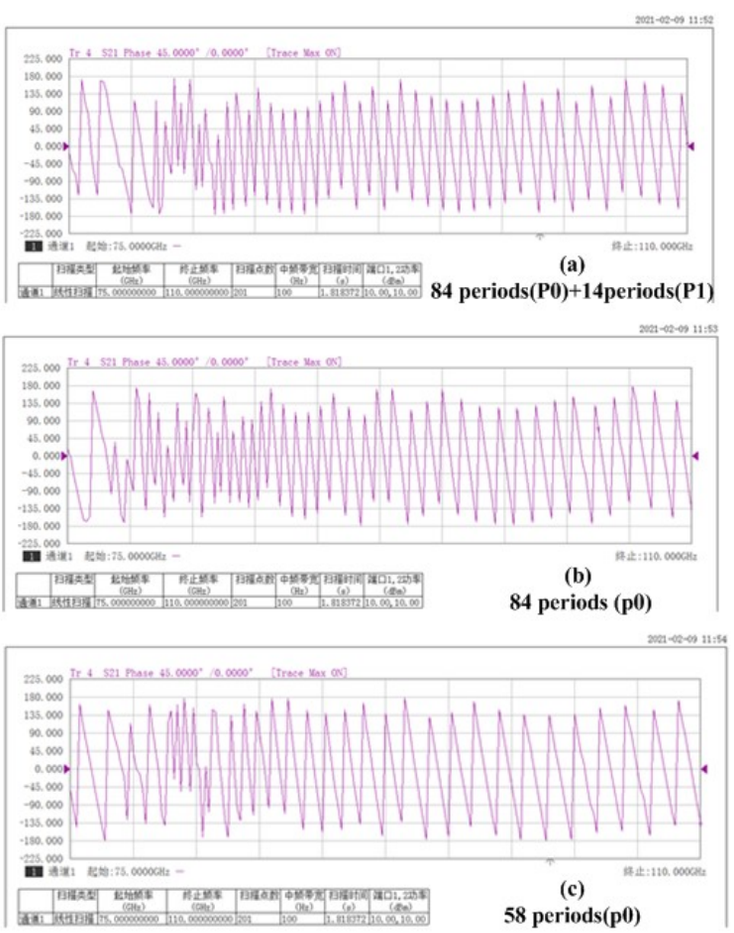

Fig. 4 Tests of transfer phase versus frequency.
图4. 测试传输相位随频率变化

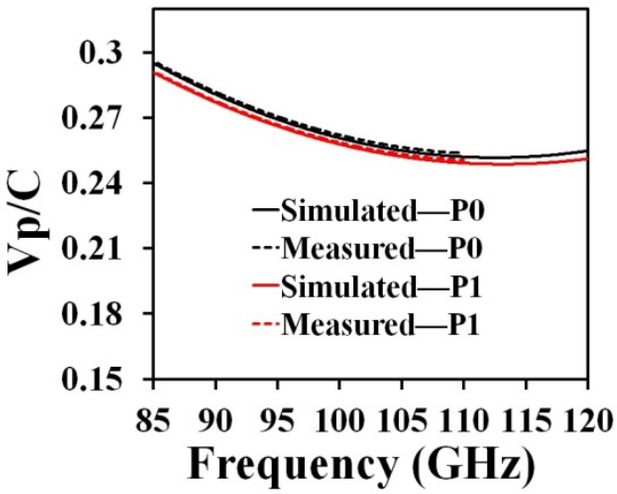

Fig. 5 Measured and simulated phase velocities for FGWs with period P_0 and P_1.
图5 测试和仿真不同半周期(P0 /P1.)曲折槽波导的相速度

simulated by using CST particle studio. According to the measured transmission loss a conductivity of $3.6*10^7$ was used in the simulation. The optimized beam voltage was found to be 19.1 kV for the FGW with half-period P_0, and the beam current was set to be 0.15 A. The cross section of the electron beam is 0.12 mm*0.45 mm. In order to ensure no electron interception on the beam tunnel, an axial uniform magnetic field of 0.5 T was used in the simulation. Fig. 6 shows the simulation model and the bunching electron beam in FGW with 14 half periods OSPVT based on the PIC. It can be seen from Fig. 6 (b) the phenomenon of electron beam bunching appears in the end of the FGW with 14 half periods OSPVT. Therefore, it is evident that some electrons are retarded and some electrons are accelerated.

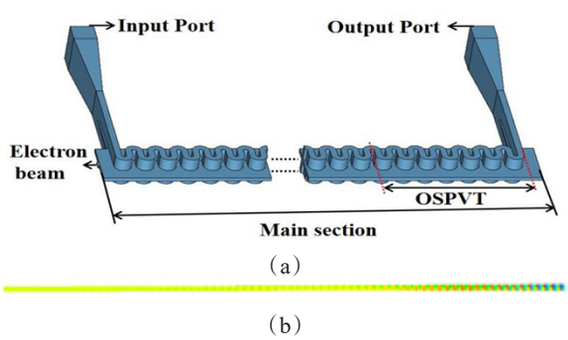

Fig. 6 (a) Simulation model of 14 half periods OSPVT based on the PIC, (b) the bunching electron beam in FGW with 14 half periods OSPVT.
图6 (a) 14个半周期带有OSPVT的PIC仿真模型,(b) 电子束群聚图

Fig. 7 shows the simulated output power as a function of input power at 95 GHz, when the total length of the FGW is set at 104 half periods under five cases, with each of them having different length of OSPVT section. It can be seen from Fig. 7 that proper selection and application of OSPVT can effectively improve the output power. Furthermore, the designed high power high efficiency FGW millimeter-wave traveling wave tube with 20*P1 OSPVT could output 240 W saturated power when the input driving signal is 0.08 W to 0.15 W. This is approximately 70 W higher than the case of without OSPVT section. When the OSPVT was set to be $14*P_1$, the saturated power and the electronic efficiency were simulated and are shown in Fig. 8. For comparison the saturated power and the electronic efficiency with the FGW OSPVT and without OSPVT are both shown in Fig. 8. In the whole frequency range of 85~110 GHz, the bandwidth of the saturated power above 100 W for the FGW with 14 half periods ($14*P_1$) OSPVT is larger than the case of without OSPVT. Fig. 8 also demonstrates that the application of OSPVT is beneficial to increase the electronic efficiency in the range of 85~110 GHz.

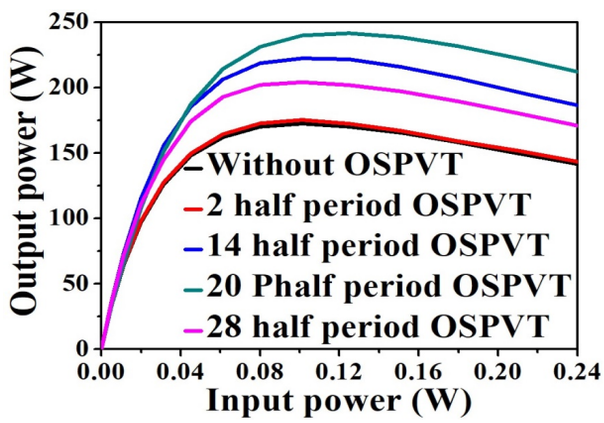

Fig. 7 Power transfer curves at 95 GHz for FGWs of different length of OSPVT
图7 不同相速跳变长度在频点95 GHz处对应输出功率曲线

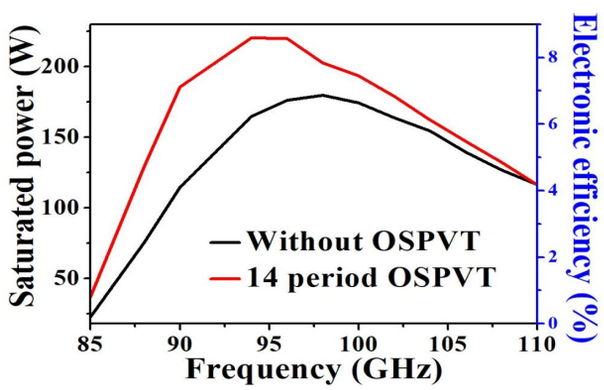

Fig. 8 Saturated output power and electron efficiency versus frequency
图8 饱和输出功率和电子效率随频率变化

4 Conclusion

In this article, an FGW millimeter-wave traveling wave tube based on OSPVT was proposed. A combination of three FGWs with and without OSPVT section, each with the same input and output couplers was fabricated. The s-parameter measurements using VNA and simulations of these FGWs OSPVT demonstrated good

transmission characteristics and wide bandwidth. Simulations predicted that the saturated power and electron efficiency were significantly improved by the application OS-PVT in the operating frequency of 85~110 GHz. It is possible that the electronic efficiency of a TWT could be further improved by more sophisticated phase velocity change techniques such as DVT and multiple stage phase velocity change, which will be studied in the future.

References

[1] Ulisse G, Krozer V. W-band traveling wave tube amplifier based on planar slow wave structure [J]. *IEEE Electron Device Letters*, 2017, **38**(1): 126-129.

[2] Abe D K, Pershing D E, Nguyen K T, *et al*. Demonstration of an S-band, 600-kW fundamental-mode multiple-beam klystron [J]. *IEEE Electron Device Letters*, 2005, **26**(8): 590-592.

[3] Suen J Y. Terabit-per-Second Satellite Links: A Path Toward Ubiquitous Terahertz Communication [J]. *J Infrared Milli Terahz Waves*, 2016, **37**(7): 615-639.

[4] Sagazio P, Callender S, Shin W, *et al*. Architecture and Circuit Choices for 5G Millimeter-Wave Beamforming Transceivers [J]. *IEEE Communications Magazine*, 2018, **56**(12): 186-192.

[5] Li X, Huang X, Mathisen S, *et al*. Design of 71 - 76 GHz Double-Corrugated Waveguide Traveling-Wave Tube for Satellite Downlink [J], *IEEE Trans on Electron Devices*, 2018, **65**(6): 2195-2200.

[6] Shvets G. Applications of electromagnetic metamaterials to vacuum electronics devices and advanced accelerators [C], Int. Vac. Electron. Conf. (IVEC). 2014, Apr: 3-3.

[7] Tucek J C, Basten M A, Gallagher D A, *et al*. Operation of a compact 1.03THz power amplifier [C], IEEE Int. Vac. Electron. Conf. (IVEC). 2016, Apr: 1-2.

[8] Tahanian E, Dadashzadeh G. A novel gap-groove folded waveguide slow-wave structure for G-band traveling-wavetube [J]. *IEEE Trans Electron Devices*, 2016, **63**(7): 2912-2918.

[9] Hou Y, Gong Y B, Xu J, *et al*. A Novel ridge-vane-loaded folded-waveguide slow-wave structure for 0.22-THz traveling-wave tube [J]. *IEEE Trans on Electron Devices*, **60**(3): 1228-1235.

[10] Sumathy M, Vinoy K J, Datta S K. Analysis of ridge-loaded folded-waveguide slow-wave structures for broadband traveling-wave tubes [J]. *IEEE Trans on electron Devices*, **57**(6): 1440-1446.

[11] Cai J, Wu X P, Feng J. A cosine-shaped vane-folded waveguide and ridge waveguide coupler [J]. *IEEE Trans on Electron Devices*. 2016, **63**(6): 2544-2549.

[12] Zheng Y, Gamzina D, Popovic B, *et al*. Electron beam transport system for 263-GHz sheet beam TWT [J]. *IEEE Trans on Electron Devices*. 2016, **63**(11): 4466-4472.

[13] Sudhamani H S, Balakrishnan J, Reddy S U M. Investigation of instabilities in a folded-waveguide sheet-beam TWT [J]. *IEEE Trans on Electron Devices*, 2017, **64**(10): 4266-4271.

[14] Lu F Y, Grieser M, Zhang C G, *et al*. 3-D Nonlinear Theory for sheet-Beam Folded-waveguide Traveling-wave Tubes [J]. *IEEE Trans on Electron Devices*, 2018, **65**(11): 5103-5110.

[15] Zhang W, Wang Y, Qu B. Design of folded double-ridged waveguide slow-wave structure [C]. IEEE International Vacuum Electronics Conference (IVEC). 2018, Apr: 1-2.

[16] Kosmahl H G. Linearized traveling wave amplifier with hard limiter characteristics [P]. 1986, U.S. patent 4 564 787, Jan. 14.

[17] Ghosh T K, Challis A J, Jacob A , *et al*. Improvements in performance of broadband helix traveling-wave tube [J]. *IEEE Trans Electron Devices*, 2008, **55**(2): 668-673.

[18] Yue Lingna, Tian Yanyan, Xu Jin, *et al*. The Folded Groove Guide, an original slow-wave structure for millimeter-wave TWT [C]. Infrared, Millimeter, and Terahertz Waves (IRMMW-THz), 2012 37th International, September: **1**-1

[19] Cho Y M, Harris I D J, Tsang D F. Theoretical and experimental characteristics of single V-groove guide for X-band and 100GHz operation [J]. *IEEE Trans on Microwave Theory and Techniques*, 1988, **36**(4).

[20] Yang H S, Ma J L, Lu Z Z. Circular groove guide for short millimeter and sub millimeter waves [J]. *IEEE Trans on Microwave Theory and Techniques*. 1995, **42**(2): 324-330.

[21] Tian Y. Y., Yue L. N., Xu J., *et al*. A novel slow-wave structure-folded rectangular groove waveguide for millimeter-wave TWT [J]. *IEEE Trans on Electron Devices*, 2011, **59**(2): 510-515.

[22] Tian Y Y, Yue L N, Zhou Q, *et al*. Investigation on sheet beam folded v-shape groove waveguide for millimeter-wave TWT [J]. *IEEE Trans on Plasma Science*, **44**(8): 1363-1368.

[23] Tian Y Y, Yue L N, Wang H X, *et al*. Investigation of ridge-loaded folded rectangular groove waveguide slow-wave structure for high-power terahertz TWT [J]. *IEEE Trans on Electron Devices*, 2018, **65**(6): 2170-2176.

[24] Tian Y Y, Yue L N, Wang H X, *et al*. High Power wideband Terahertz Traveling wave Tube Based on Folded Double Ridge Groove waveguide [J]. *J. Infrared Millim. Waves*, 2018, **37**(6): 711-716.

[25] Jr Gilmour A S, Ebrary I. Klystrons, Traveling Wave Tubes, Magnetrons, Crossed-Field Amplifiers, and Gyrotrons [M]. 2011, Artech house, 2011, 317-345,